PLANAR ELECTRON SOURCES AND THE ELECTRON TRAP ELTRAP

M. Cavenago*, INFN-LNL, Legnaro, Italy; G. Bettega, F. Cavaliere,
A. Illiberi, R. Pozzoli, M. Romé, L. Serafini, INFN-Milano and Univ. Milano, Italy

Abstract

A Malmberg-Penning trap, named ELTRAP, installed and operated at the University of Milan, is briefly described; trap length ranges from 10 cm to 1 m; an uniform magnetic field confines electron radially. Several experimental regimes were investigated with the internal CW planar electron source: plasma, beam-plasma, beam, depending on the injection/extraction method chosen. Dynamics of intense electron beams may be simulated in this machine. Evolution of electron vortices and virtual cathode formation is documented. Machine upgrading are discussed: an external laser pulsed electron source will make also experiments of bunch expansion possible; larger plasma will be studied with planar sources under construction.

INTRODUCTION

Malmberg-Penning traps represent a simple, yet effective and flexible, device for the accumulation of electron beams, making a cylindrically shaped cloud, where several non-linear and self-organization effects can be conveniently studied [1].

The design of ELTRAP machine, now installed at University of Milan, aimed at providing a large size Malmberg-Penning trap (inner electron diameter $2r_w = 90$ mm, plasma length up to 1 m), and an adequately uniform field. Interesting results, obtained with a standard electron source (diameter $2r_f = 25$ mm), and design issue and development of a larger source (70 mm) are here described (see Fig. 1); these thermionic sources operates inside the main solenoid field. Another e$^-$ source, capable of ns bunch thanks to laser drive, is being built, and will be mounted externally (see Fig. 2).

Filamentation and other major space charge effects of intense e$^-$ beams, found for example in rf photoinjectors (beam energy 1 MeV, current 100 A), are easily studied in this machine, notwithstanding the low voltage ($0.01 - 0.1$ kV), by keeping the same perveance order.

Along trap axis z, electrons are confined by an electric potential $\phi(x, y, z; t)$, whose z profile is adjustable by 12 electrodes; in particular the negatively biased electrode (-80 V) that reflect electrons are named plug electrodes; $\phi = 0$ is by convention the vacuum chamber, usually connected also to central electrodes. Radial motion is effectively prevented by the solenoid field $\mathbf{B} \cong B_c(z)\hat{z}$, which adds a slow drift $\mathbf{v}_d = (\mathbf{E} \times \mathbf{B})/B^2$ to the electron motion, where $\mathbf{E}$ included the self-fields, which dominate the rotation.

* cavenago@lnl.infn.it

Note indeed that the internal sources are immersed in the solenoid field $B_c(z_s) \cong B_0$, where z_s is the source position and B_0 is the middle plane field $B_0 = B_c(0)$, so Busch rotation is negligible even at large radius [2]; the external source has conveniently small radius (≤ 2.5 mm and of laser spot).

The internal source is a filament (or a spiral) directly heated by a current I_f. Let I_s be the total current leaving the source assembly and V_b the source center applied voltage: $V_b = -\phi(0, 0, z_s)$. Let us define the filament voltage $V_f = \phi(0, r_f, z_s) - \phi(0, 0, z_s)$. Even with a small source $r_f = 12.5$ mm, a large beam perveance P_b is typically obtained ($P_b = 5$ microperv with $I_s = 0.4$ mA and $V_b = 20$ V and $V_f = 3$ V).

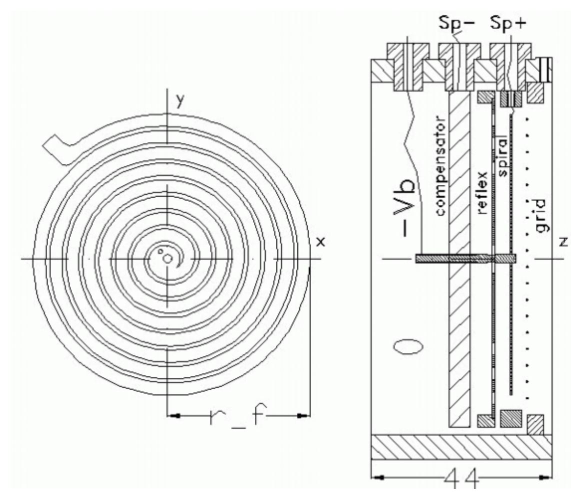

Figure 1: Internal e source with planar spiral emitting surface of radius r_f; heating current I_f flows from contact SP+ to SP- via the spiral and the compensator; V_b is also sensed.

BEAM PRODUCTION AND INJECTION

Basic theory of evolution of stored plasma (vorticity-line density equivalence, 2D inviscid motion) were discussed elsewhere [1], so we consider here the injection phase, when the first plug is off. Even if current is emitted in all directions, note that $j_r \ll j_z$ for the presence of B_0; let us assume that B_0 is strong enough so that the electron gyroradius is negligible compared to r_f and r_w. Near the source, as a first approximation, it is convenient to average over the azimuthal coordinate ϑ, since the electrodes are cylindrical and $B_\vartheta = 0$; let $\bar{g} = (1/2\pi) \int \mathrm{d}\vartheta\, g$ and $\tilde{g} = g - \bar{g}$ for any g. Moreover, let be $j_s(\vartheta, r)$ the [z-component of] the current emitted by source and $j_a = \bar{j}_s$; representing

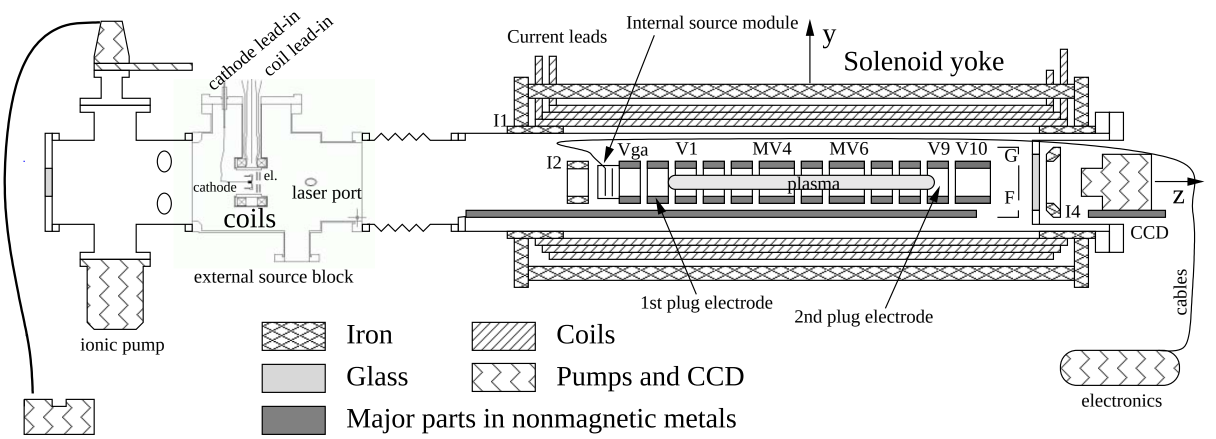

Figure 2: Experimental set-up general plan (only one source plug-in or the external source can be used at a time); vertical section. I1,I2,I3 and I4 are shims to improve **B** uniformity, MV4 and MV6 sectored electrodes, F the phosphor screen with its guard ring G. A UV laser, making a 40^0 angle with z axis enters through a CF16 quartz window and via a laser port and some holes in the extraction electrodes (el.) reachs a pre-heated cathode

j_s faithfully would require actually to conform to the filament shape, while $j_a(r)$ is roughly uniform :$j_a = -j_{\text{th}}$ for $r < r_f$. Similarly the average $\phi_a = \bar{\phi}|_{z_s}$ of the potential at the source is simply determined by the Ohm law applied to the filament as

$$\bar{\phi} \cong \phi_a(x,y) = -(V_b - V_f r^2/r_f^2) \tag{1}$$

The Poisson equation and continuity equation give

$$\triangle\bar{\phi} = -\frac{e\bar{n}F}{\epsilon_0} = \frac{j_{\text{th}}F\sqrt{m}}{\epsilon_0\sqrt{2e(\bar{\phi}-\phi_a)}} \tag{2}$$

for $\bar{\phi} > \phi_a$ and $r < r_f$; and 0 otherwise. The reflection factor $F(r)$ is $F = 1$ if the beamlet is not reflected (that is, travels along z until it is absorbed by the phosphor screen) and $F = 2$ if it is reflected (for example, this happens always if the end plug is on). Eq. 1 and 2 and F and electrodes voltages define a nonlinear elliptic problem for ϕ. For example, requiring a uniform beam density in the central drift region (where $\phi = 0$ at $r = r_w$) implies $\phi - \phi_a$ =const (in other words equal speed $|v_z|$); so $\phi = -V_c + V_f(r/r_f)^2$ for $r < r_f$. Then we get $V_c = -V_f[1 + 2\log(r_w/r_f)]$ and a matching condition

$$j_{\text{th}} = j_{\text{th}}^m = \frac{4\epsilon_0 V_f}{F r_f^2}\sqrt{\frac{2e[V_b - (1+2\log(r_w/r_f)V_f]}{m}}, \tag{3}$$

similar to a Child-Langmuir condition, for the average thermionic current, with the typical power $V^{3/2}$ scaling in the voltages.

Further analysis shows that if $j_{\text{th}} < j_{\text{th}}^m$ the beam speed is higher at the center; while if $j_{\text{th}} \gg j_{\text{th}}^m$ a virtual cathode and a hollow beam are formed. In that case, Eq. 3 may show an hysteresis effect if F becomes 2. Note that grid has an auxiliary role: grid speeds up the beam after emission, but, since energy is conserved, it can not change the speed of beam inside the central drift electrode and therefore the eq. 3 match.

The vortex evolution region

Especially in the case of an hollow beam, the azimuthal perturbation (induced by grid and source asymmetry) may grow along z, indeed vortices are visible on the phosphor screen.

If all electrodes are held to $\phi = 0$, the convenient first approximation is $\partial_z E_z \cong 0$, so vorticity-density relation is recovered (that is $\zeta = \text{curl}_z\mathbf{v} \cong en/\epsilon_0 B_0$) and in stationary regimes

$$\partial_z n = -\frac{\mathbf{v}_\perp}{v_z}\cdot\nabla n \quad , \quad \mathbf{v}_\perp = \frac{\mathbf{B}\times\text{grad}\phi}{B_0^2} \tag{4}$$

which gives vortex evolution with z. In particular, screen display depends on $L/(v_z B_0)$, with $L = z_p - z_s$ and z_p the phosphor position.

Internal planar source

It is easily shown (for example [3], Eq. 1 and 2) that generating a large radius thermionic plasma ($r > 2$ cm) with a reasonable power $P_f = I_f V_f < 200$ W implies a low work function $\phi_e < 2.5$ eV; that requires some cathode development. Fairly satisfying results were obtained with W/Ce filaments, limited to a few turns. On the other side, large planar spirals made of porous tungsten were built, and several impregnation methods are being considered (similar to the usual type B, a mixture of barium and calcium aluminates, [4], $\phi_e \cong 2$ eV), also in consideration of the particular geometry.

The planar source is to be mounted inside a 44 mm long copper cylinder, which fits into one end of guard electrode Vga; so source heat distributes on a large surface, as verified with the 25 mm diameter source, which has the same mounting interface. The maximum grid transparency reaches 97 %. Some transparencies is also lost, when additional supports to prevent sagging of the spiral are mounted.

Laser enhanced source

In the laser enhanced source concept [6], a laser impinges onto the surface of a thermionic emitter, heated at $T_s \cong 800\ ^0\mathrm{C}$, below its operational temperature T_o ($T_o = 1000$ to 1200 ^{0}C in the design example of type B-311 cathode). This surface condition enhances efficiency of photoelectric emission, so that moderate energy (0.3 mJ) lasers are required for reasonable charge $\int \mathrm{d}t\, I_s \cong 50$ pC. Due to small source radius, commercial dispenser cathodes are available and use limited power ($P_f = 15$ W at $T_o = 1200\,^0\mathrm{C}$).

The cathode is placed in the middle of an Helmholtz coil pair, where $z' = 0$; a magnetic field $B_1(z')$ is still useful to focus electrons at the begin of the acceleration gap; B_1 can be raised to 500 G, with a 0.5 % uniformity over a distance $z' < z_1 = 13$ mm from cathode. By reversing current in one coil, $B_1 \cong b_1 z'$ with $b_1 \cong 100$ G/cm may also be obtained.

For this source the operation voltage is much higher $V_b \cong -10$ kV, so that longitudinal bunching is well preserved. The cathode is covered by an approximate Pierce electrode, and two anodes complete the triode arrangement, for flexibility of operation. Relation between I_s, B_1 and V_b will be studied first; for example it is expected that increasing B_1 limits the transverse space available to electrons, and therefore I_s.

EXPERIMENTAL REGIMES

According to the temporal schedule of the plug electrodes, we have three regimes. In the plasma regime, the first plug is held off ($\phi = 0$) temporarily, so that electrons travel through all electrode to the second plug, and are reflected back; turning the first plug on separates the stored plasma from the electron source. With particular tuning of V_b, I_s and B_0 transient instabilities may be observed with sectored electrodes pick-ups [5]. By turning the second plug off after a prescribed time t_s, the stored electrons are dumped on the phosphor screen, where line density profile $n_s(x, y; t_s)$ is measured by scintillation and a CCD camera and total charge Q_s by a calibrated amplifier. Changing t_s allows to reconstruct a movie of the n_s evolution; coherent structure motion and long confinement times $\tau_s \equiv -1/(\mathrm{d}\log Q_s/\mathrm{d}t_s)$ are usually observed [1]. Analogy of structures with meteorology and with astrophysical plasma is striking.

The beam-plasma regime is obtained by leaving the first plug off and the second plug on continuously: so electron travels up the second plug, are reflected back, and lost through the source, while the self-consistent potential ϕ keep memory of the plasma evolution (eq. 2 or its 3D analogue). Instabilities and particular bands of V_b values can be clearly related, in purely stationary regimes. Since no electron may reach the phosphor screen, up to now the only diagnostic are the electrode pickups [7].

In the beam (or drift) regime, both plugs are held off continuously. Depending on I_s, a virtual cathode may form, which lead to an hollow beam (eq. 3). From the phosfor screen image, structures of the beam density $n_b(x, y, B_0)$ are found; thanks to eq. 4, decreasing B_0 is roughly equivalent to increasing the drift length L or the transit time t_t. Evolution of n_b with t_t can be rapidly observed, also thanks to improvements in CCD read-out (see Fig. 3).

Figure 3: Vortex and hollow beam formation, before $B_0 = 500$ G is decreased slowly, with $j_{th} = 2.2\ \mathrm{A/m^2}$, and $L = 1.1$ m; full movie at Ref. [7]

Simulation of these instabilities and structure with PIC (particle in cell) codes is described elsewhere [8]. Before a complete theorical systematization of results, the question of accumulated ion density should be raised.

We developed an experimental technique, based on 'clearing fields': between plugs, E_z is not held zero always, but is pulsed to a few V/m, for periods from $t_p = 100$ to 900 ms long, comparable to instability rising times. In other words, $\phi \cong a_0(t) + a_1(t)z$ with $a_0, a_1 L \ll V_b$, so that perturbation of electron motion is small [in particular the bouncing period t_b variation $\delta \log t_b = O(a_0/V_b)$ can be zeroed], but ions are pushed into the plugs, where they are separated and shielded from electron self-fields. Instabilities are largely affected and often suppressed, which is a preliminary evidence of ion role in this instabilities.

REFERENCES

[1] D. H. E. Dubin and T. M. O'Neil, Rev. Modern Physics 71 (1999) 87.

[2] J.R. Pierce, *Theory and Design of Electron Beams*, Van Nostrand, Princetown (1954), 175-181.

[3] Amoretti et al., Rev. Sci. Instrum. 74 (2004) 1991

[4] G. A. Haas, in *Methods of experimental physics*, vol. 4A, p. 1 (Academic Press, New York, 1967).

[5] Bettega et al., in *Non-Neutral Plasma Physics V*, AIP, Melville NY, (2003), 50

[6] B. Leblond, Nucl. Instrum. Meth. A317 (1992) 365

[7] http://pc3eltrap.mi.infn.it/~eltrap

[8] G. Bettega et al., Appl. Phys. Lett., 84 (2004) 3807